

Planar Monopole UWB Antenna with Cuts at the Edges and Two Parasitic Loops

Karlo Q. da Costa, Victor Dmitriev
Federal University of Para, Belém, Para, Brazil
E-mails: karlo@ufpa.br, victor@ufpa.br

Abstract— In this paper, we analyze an antenna for application in ultra wideband systems. This antenna is composed by one planar monopole with cuts at the edges and two parasitic loops. The numerical analysis of the antenna was done by the Method of Moments (MoM). For comparison, some of the calculations were also made by the commercial software IE3D. The results of this analysis show that the antenna has excellent impedance matching in all frequency range of UWB systems.

Index Terms— UWB antenna, planar monopole antenna, numerical analysis, Method of Moments (MoM).

I. INTRODUCTION

In ultra wideband (UWB) systems, extremely short pulses are used. These pulses can provide data with high bit rate. They usually occupy ultra wide band in the frequency domain. The spectrum of frequencies reserved for these systems is 3.1-10.6GHz. Examples of UWB signal applications are communications, radar and imaging systems [1], [2].

Planar antennas are widely used in UWB systems because of their low cost of fabrication, low size, and simple structure. Some examples of conventional planar monopoles antennas with rectangular, triangular and circular geometries are presented in [3]. One of the deficiencies of the rectangular monopole is its relatively small matching bandwidth which is about 80% [4]. This value is smaller than the full bandwidth of the UWB systems, which is 110% (the frequency range is 3.1-10.6 GHz).

Some techniques can be used to enlarge the bandwidth of planar monopole antenna [5]-[9]. For this purpose, modifications of the ground plane and a T aperture in the geometry of the antenna were made [5]. In [6], a monopole planar antenna with a folded patch was used. A rectangular planar monopole antenna combined with two parasitic loops was suggested in [7] and antennas with elliptical geometries were analyzed in [8].

In this work, we analyze a planar UWB antenna with cuts at the edges of a metal rectangle and two parasitic loops. This is a modified version of the antennas presented in [7] and [9]. To enlarge the matching bandwidth, the dimensions of the antenna were optimized with cut-and try method. For the numerical analysis, a Method of Moments (MoM) code was developed. For comparison with the developed code, some calculations were made also with the software IE3D [11].

II. GEOMETRY OF THE ANTENNA

Fig. 1 shows the geometry of the proposed antenna. In this figure, L is the width of the antenna and $H+W$ is the height of the patch with respect to the ground plane. The parameter s is the width of the feeding transmission line which connects the patch with the inner conductor of the coaxial cable. The dimensions of the rectangular cuts at the edges of the antenna are w_1 - w_6 . The dimensions of the loops are W_1 e L_1 and their widths are r_1 e r_2 . The distance between the loops and the monopole is d . Notice that the geometry of this antenna is symmetrical with respect to the plane $x=L/2$.

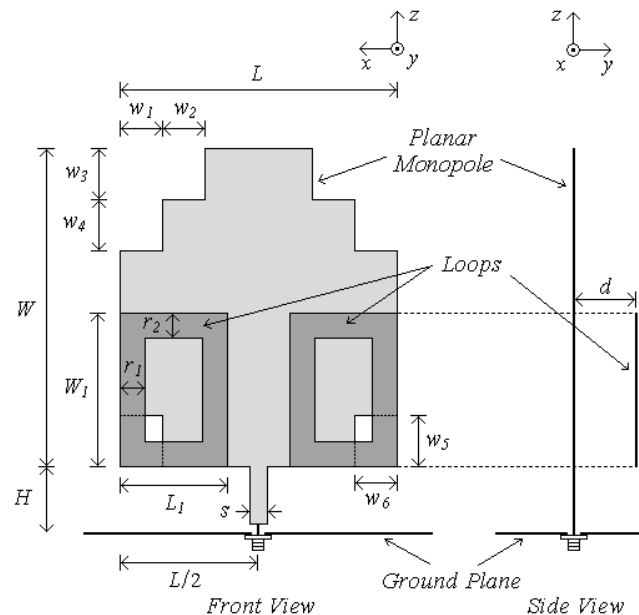


Fig. 1. Geometry of the proposed UWB planar monopole with cuts at the edges and two loops.

III. MATHEMATICAL MODEL

A. Integral equation of the electric field

The mathematical model of the antenna on Fig. 1 was realized by the integral equation for electromagnetic potentials in the frequency domain with the temporal dependence $\exp(j\omega t)$ [12]:

$$\bar{E}_r = -j\omega\mu_0 \iint_S \bar{J} \frac{e^{-jkR}}{4\pi R} ds' + \nabla \left[\frac{1}{j\omega\epsilon_0} \iint_S \nabla \cdot \bar{J} \frac{e^{-jkR}}{4\pi R} ds' \right] \quad (1)$$

where \bar{E}_r (V/m) is the electric field radiated by a current density \bar{J} (A/m) on the conductors of the antenna. This current will appear when the antenna is fed by a coaxial cable connected at the point $x=L/2$ (Fig. 1). The parameter S represents the superficial area of the antenna, j is imaginary unit, $k=\omega(\mu_0\epsilon_0)^{1/2}$, ω is the angular frequency (rad/s), μ_0 and ϵ_0 are the magnetic permeability and electrical permittivity, respectively of the free space, and R is the distance between one point on S and one observation point near the antenna.

B. Numerical solution by MoM

The numerical MoM solution of (1) presented in this section is explained by using example of the rectangular monopole antenna (Fig. 2). With minor modifications in the geometry, this model is used to analyze the proposed UWB antenna (Fig. 1).

The problem to be solved here is to find the current distribution \bar{J} in (1) when a given external electric field \bar{E}_i is falling on the antenna. This incident field represents the source of the problem. The conductors of the antenna are considered lossless. In this case, the boundary condition on S is $(\bar{E}_r + \bar{E}_i) \cdot \bar{a}_t = 0$, where \bar{a}_t is a tangential unity vector on S . To solve this problem by MoM [10], the following approximations are firstly established:

$$\bar{J} = \sum_{n=1}^{N_x-1} \sum_{m=1}^{N_z} J_x^{n,m} P_{J_x}^{n,m} \bar{a}_x + \sum_{n=1}^{N_x} \sum_{m=1}^{N_z-1} J_z^{n,m} P_{J_z}^{n,m} \bar{a}_z \tag{2}$$

$$\nabla \cdot \bar{J} = -\frac{1}{j\omega} \sum_{n=1}^{N_x} \sum_{m=1}^{N_z} \left[\frac{J_x^{n,m} - J_x^{n-1,m}}{\Delta x} + \frac{J_z^{n,m} - J_z^{n,m-1}}{\Delta z} \right] P_{\sigma}^{n,m} \tag{3}$$

where

$$P_{J_x}^{n,m} = \begin{cases} 1, & x_{n-1/2} < x < x_{n+1/2} \text{ and } z_{m-1} < z < z_m \\ 0, & \text{otherwise} \end{cases} \tag{4}$$

$$P_{J_z}^{n,m} = \begin{cases} 1, & z_{m-1/2} < z < z_{m+1/2} \text{ and } x_{n-1} < x < x_n \\ 0, & \text{otherwise} \end{cases} \tag{5}$$

$$P_{\sigma}^{n,m} = \begin{cases} 1, & x_{n-1} < x < x_n \text{ and } z_{m-1} < z < z_m \\ 0, & \text{otherwise} \end{cases} \tag{6}$$

The parameters N_x and N_z are the numbers of division along x and z directions respectively, and $\Delta x=L/N_x$, $\Delta z=W/N_z$. Fig. 2 shows the grid of discretization for the rectangular antenna. The functions (4)-(6) are defined in this grid.

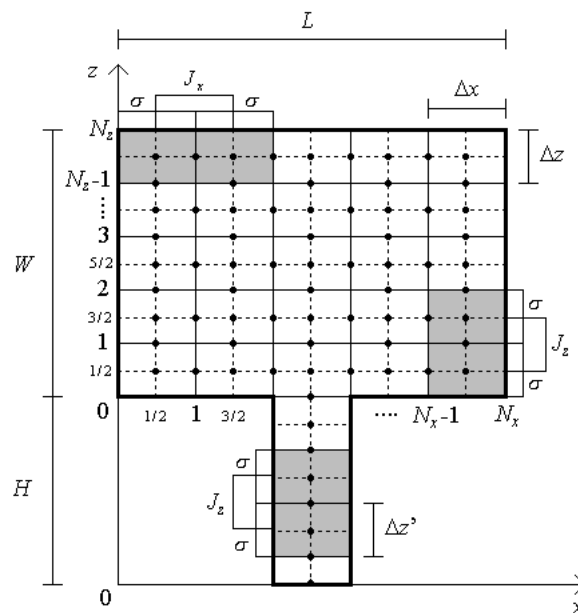


Fig. 2. Details of the MoM discretization for the conventional rectangular antenna.

Fig. 3 shows geometrical details used in each current element of index I inside the grid in Fig. 2. In this figure, the direction of P_I^- to P_I^+ is parallel to an axis of the coordinate system ($+x$ or $+z$). Inserting (2) and (3) into (1), using the boundary condition and calculating the integral in one segment Δl_J , which connects the points P_J^- and P_J^+ , the following equation can be obtained:

$$\int_{\Delta l_J} \bar{E}_i \cdot \bar{dl} = \sum_{I=1}^{N_I} J_I \left[j\omega\mu_0 \Phi \bar{\Delta l}_I \cdot \bar{\Delta l}_J + \frac{1}{j\omega\epsilon_0} (\Phi^{++} - \Phi^{-+} - \Phi^{+-} + \Phi^{--}) \right] \quad (7)$$

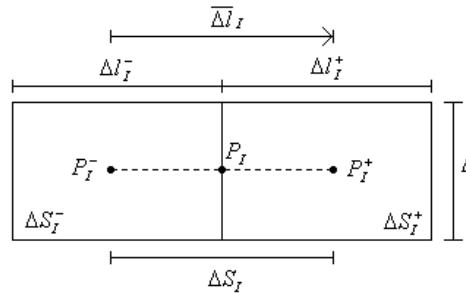


Fig. 3. Geometry of one generic current element of the grid in Fig. 2.

where $N_I = (N_x - 1) \times (N_z) + (N_z - 1) \times (N_x) + N_h$ is the total number of unknowns J_I , and N_h is the number of segments on the height H . The current density J_I can be $J_x^{n,m}$ or $J_z^{n,m}$ in (2) and (3). The functions Φ are the mutual interactions between the elements I and J . These functions are calculated by the following expressions:

$$\Phi = \frac{1}{\Delta l_I} \iint_{\Delta S_I} \frac{e^{-jkR_{IJ}}}{4\pi R_{IJ}} ds' \Bigg|_{P_I^-}^{P_I^+} \quad (8)$$

$$\Phi^{++} = \frac{1}{\Delta l_I^+} \iint_{\Delta S_I^+} \frac{e^{-jkR_{IJ}^{++}}}{4\pi R_{IJ}^{++}} ds' \Bigg|_{P_I^+}^{P_I^+} \quad (9)$$

$$\Phi^{+-} = \frac{1}{\Delta l_I^+} \iint_{\Delta S_I^+} \frac{e^{-jkR_{IJ}^{+-}}}{4\pi R_{IJ}^{+-}} ds' \Bigg|_{P_I^+}^{P_I^-} \quad (10)$$

$$\Phi^{-+} = \frac{1}{\Delta l_I^-} \iint_{\Delta S_I^-} \frac{e^{-jkR_{IJ}^{-+}}}{4\pi R_{IJ}^{-+}} ds' \Bigg|_{P_I^-}^{P_I^+} \quad (11)$$

$$\Phi^{--} = \frac{1}{\Delta l_I^-} \iint_{\Delta S_I^-} \frac{e^{-jkR_{IJ}^{--}}}{4\pi R_{IJ}^{--}} ds' \Bigg|_{P_I^-}^{P_I^-} \quad (12)$$

The variables R in (8)-(12) are the mutual distances between the points (+ or -) of the current element I to the points (+ or -) of the current element J . If $kR \ll 1$, the following approximations can be used:

$$\Phi = \frac{1}{4\pi\Delta l} \left[\Delta l \times \ln \frac{(\sqrt{\Delta l^2 + \Delta^2} + \Delta)}{(\sqrt{\Delta l^2 + \Delta^2} - \Delta)} + \Delta \times \ln \frac{(\sqrt{\Delta l^2 + \Delta^2} + \Delta l)}{(\sqrt{\Delta l^2 + \Delta^2} - \Delta l)} - jk\Delta l \times \Delta \right] \text{ if } I = J \quad (13)$$

$$\Phi = \frac{1}{4\pi\Delta l} \frac{e^{-jkR}}{R} (\Delta l \times \Delta) \quad \text{if } I \neq J \quad (14)$$

The left side of (7) means a voltage ΔV applied between the points P_J^- and P_J^+ . When (7) is desolved for $J=1, 2, \dots, N_r$, a linear system of order N_r is obtained. The solutions of this system, for a given excitation field \bar{E}_i , produce the total current density of the antenna \bar{J} .

The ground plane is modeled by infinite and perfect conductor, therefore one can use the image theory. The coaxial cable is modeled by a delta gap $\Delta V=1V$ between the ground plane and antenna. This voltage is applied in the first segment of the dimension H of the antenna, near the ground plane (Fig. 2). With this feeding, the voltages of the other segments are null.

The rectangular loops were modeled by striplines with one-dimensional current density. This current possesses component J_x for the segments along the direction x and J_z for the segments along the direction z . For thin loops, it is a good approximation. The total number of current elements of the loops is N_e , and the total number of current elements of the antenna is $N_r=(N_x-1)\times(N_z)+(N_z-1)\times(N_x)+N_h+N_e$.

IV. NUMERICAL RESULTS

A MoM code based on the theory presented in previous sections was developed in this work. With this computational program, several simulations were made. Some of the geometrical parameters such as $(w_i, i=1,2,\dots,6)$, W_1 , L_1 , r_1 , r_2 and d , were varying, and other dimensions of the antenna such as $L=18$, $W=25$, $H=1.25$ and $s=2$ were fixed (all dimensions are given in millimeters). From the results of these simulations, it was observed that the dimensions of the cuts and the loops which give better results are $w_1=w_2=w_6=3\text{mm}$, $w_3=w_4=w_5=4\text{mm}$, $W_1=14\text{mm}$, $L_1=8\text{mm}$, $r_1=r_2=2\text{mm}$ and $d=6\text{mm}$. The results presented below are calculated for antennas with these optimized dimensions.

In all simulations with the developed code, the discretization with square cells $\Delta z=\Delta x=1\text{mm}$ was used. In this case, the antenna with cuts and two loops has the parameter $N_r=725$. In the simulations done with the software IE3D, a convergence criteria of $\lambda/20$ in $F=15\text{GHz}$, where λ is the wavelength and F the operation frequency was used.

A. Input impedance and reflection coefficient

Figs. 4 and 5 show the input impedance ($Z_{in}=R+jX$) of the planar monopole of Fig. 1 with and without loops, respectively. The antenna without loops has the same dimensions as ones of the antenna with loops. These results were obtained with the developed MoM code and the software IE3D. One can note a good agreement between them.

We see in these figures, that the principal difference between the two antennas is near $F=6.5\text{GHz}$. Due to the loops, the real part of the input impedance R varies less with frequency around the value of

50Ω, and the imaginary part of the input impedance X is closer to zero. This produces a better input matching of the antenna with a transmission line with characteristic impedance 50Ω.

Notice also that the regions of frequencies near $F=4$ GHz and 8 GHz correspond, respectively, to the $\lambda/4$ and $\lambda/2$ modes of the antenna along the axis z . The current distribution for these modes will be presented in the next section.

Figs. 6 and 7 show, respectively, the reflection coefficient of the antenna in Fig. 1 without and with loops. This parameter was calculated by the expression $\Gamma=20\log(\text{abs}((Z_{in}-Z_0)/(Z_{in}+Z_0)))$, where $Z_0=50\Omega$ is the characteristic impedance of the feeding transmission line. For comparison, we presented in these figures the reflection coefficient of the conventional rectangular planar monopole with the same dimensions $L=18$, $W=25$, $H=1.25$ and $s=2$, all dimensions are in millimeters.

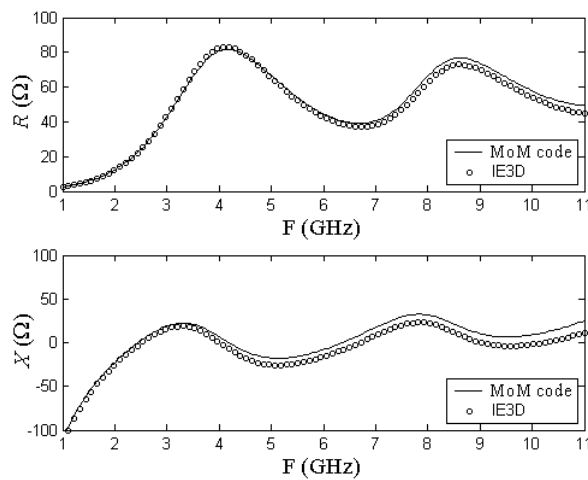


Fig. 4. Z_{in} of the antenna in Fig. 1 without loops.

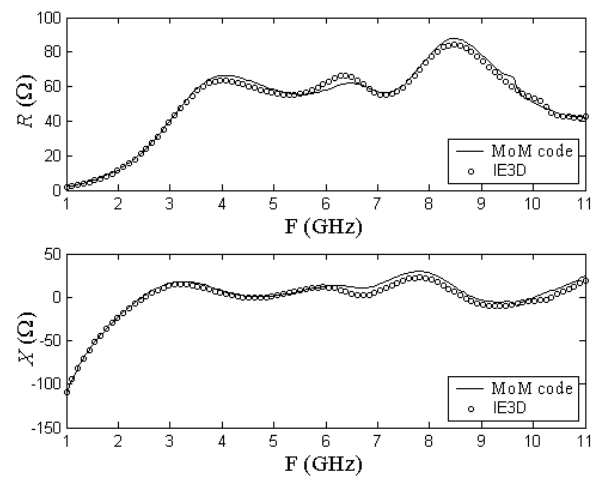


Fig. 5. Z_{in} of the antenna in Fig. 1 with two loops.

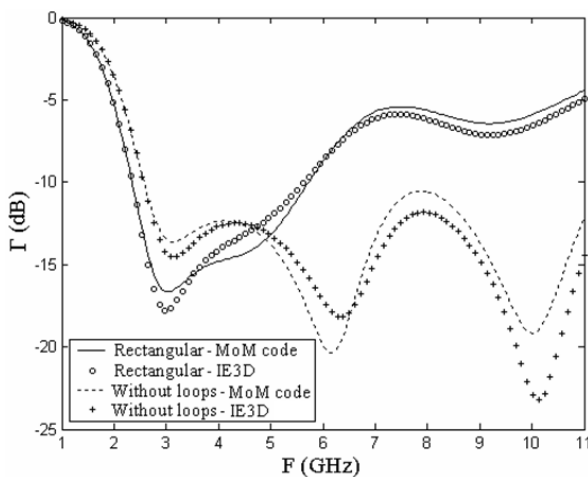


Fig. 6. Reflection coefficient of the rectangular planar antenna and of the modified one (Fig. 1).

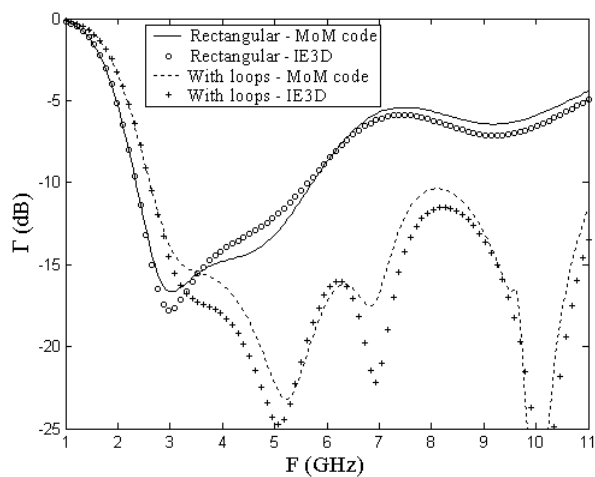


Fig. 7. Reflection coefficient of the rectangular planar antenna and of the modified one (Fig. 1).

From these figures, one can observe that the conventional rectangular monopole antenna has a bandwidth near the 80%, which does not cover the whole frequencies of UWB systems. The antennas

with cuts (with and without loops) possess impedance matching ($\Gamma < -10\text{dB}$) in the range of frequencies of UWB systems (3.1-10.6 GHz). But only the antenna with cuts at the edges and two loops has the reflection coefficient $\Gamma < -15\text{dB}$ in the frequency range 3-7GHz (Fig. 7). Thus, the antenna with loops possesses a better impedance matching.

B. Current distribution

Fig. 8 presents examples of current distribution on the surface of the antenna with cuts and two loops at the frequencies $F=4$ and 8GHz obtained by the MoM code. These current distributions are similar to that of the resonant modes with $\lambda/4$ and $\lambda/2$, which are characteristics of the rectangular planar monopole antenna.

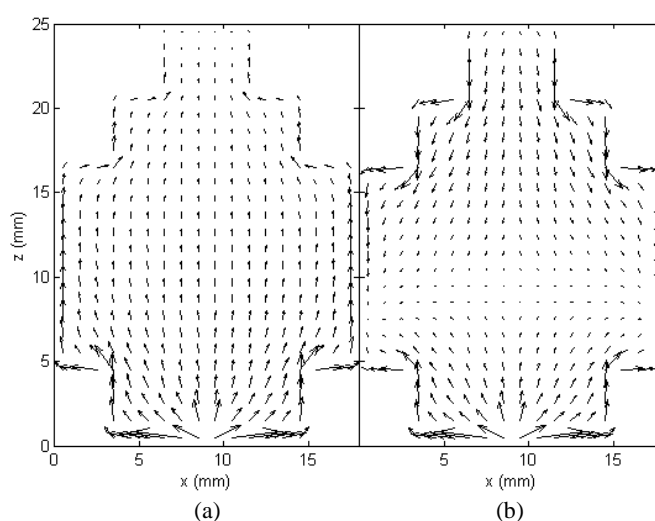


Fig. 8. Examples of current distribution of the antenna with cuts and loops: $F=4$ GHz (a), $F=8$ GHz (b).

C. Radiation diagrams

Figs. 9-12 show the radiation diagrams of the antenna with cuts and two loops for the frequencies $F=2.5, 5.0, 7.5$ and 10.0 GHz. The results were calculated by the MoM code and by the software IE3D. One can see a good agreement between them.

These figures present the radiation diagrams in the planes xz and yz . The horizontal diagrams in the plane xy are omnidirectional in the inferior band (3-5GHz), but they have a small directionality in the upper band (5-10GHz). These results are explained by asymmetry of the antenna's geometry in this plane, because there are two loops only in front of the antenna in the plane $y=d$ (Fig. 1). With two loops placed symmetrically at the other side of the antenna in the plane $y=-d$, the diagram could be symmetrical for all frequencies of the band 3-10GHz.

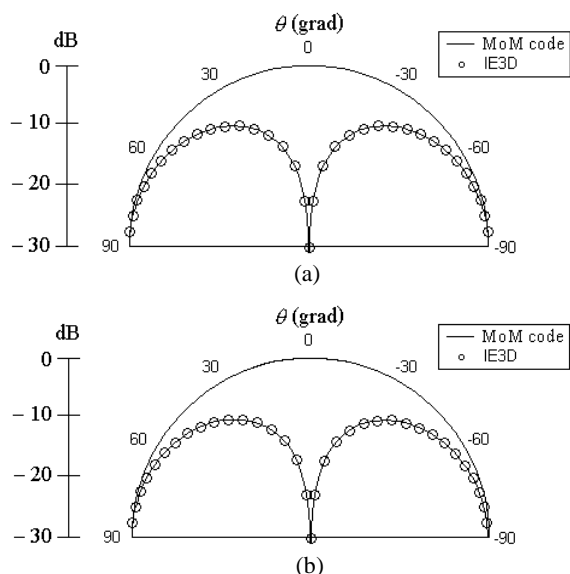


Fig. 9. Radiation diagrams of the antenna with cuts and two loops, $F=2.5\text{GHz}$: plane xz (a), plane yz (b).

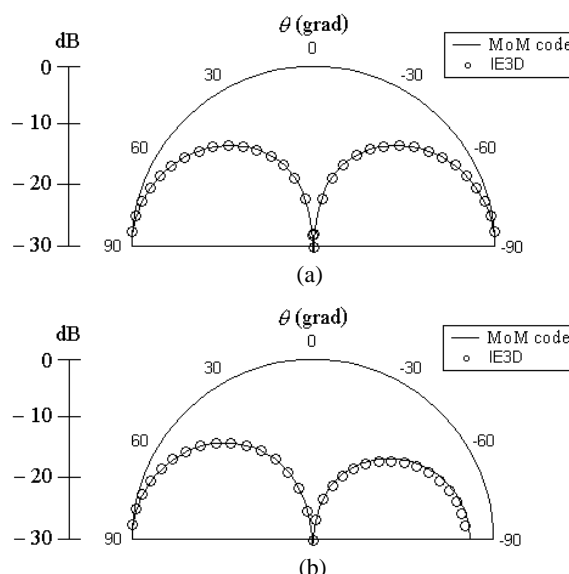


Fig. 10. Radiation diagrams of the antenna with cuts and two loops, $F=5\text{GHz}$: plane xz (a), plane yz (b).

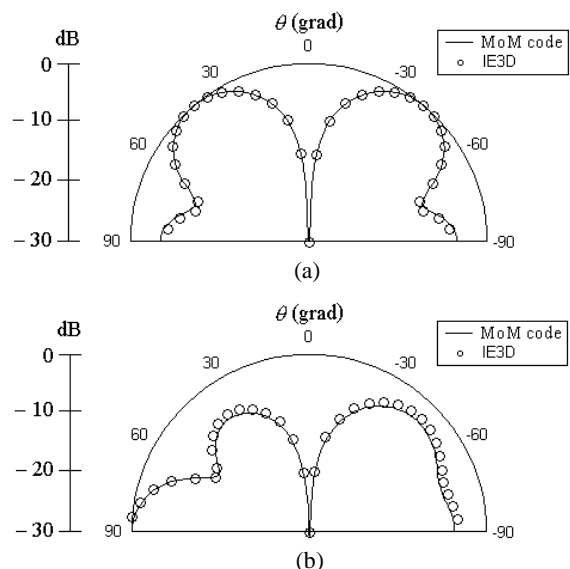


Fig. 11. Radiation diagrams of the antenna with cuts and two loops, $F=7.5\text{GHz}$: plane xz (a), plane yz (b).

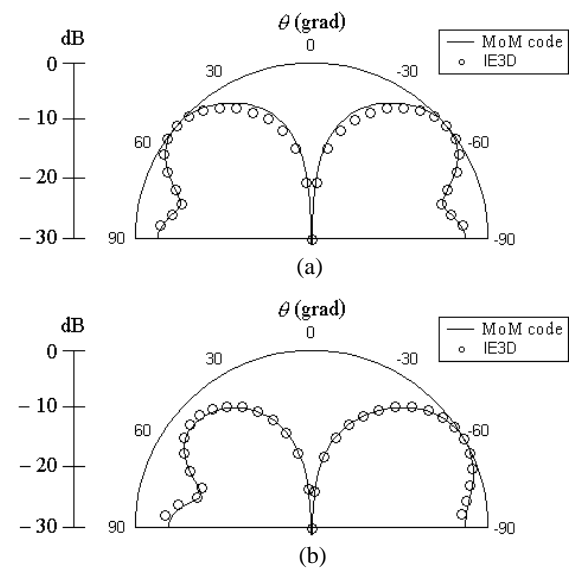


Fig. 12. Radiation diagrams of the antenna with cuts and two loops, $F=10\text{GHz}$: plane xz (a), plane yz (b).

V. CONCLUSIONS

This work presented an antenna with good input matching and radiation diagrams in all range of frequencies of UWB systems. The antenna is a rectangular planar monopole with cuts at the edges and two parasitic loops. The analysis of this antenna was done by the developed MoM code and by the software IE3D. The results obtained by these programs have a good agreement. One proposal for future work is the analysis of the antenna with cuts at the edges and four parasitic loops placed symmetrically with respect to the plane xy in order to improve the radiation diagram of the antenna.

ACKNOWLEDGMENT

This work was supported by the Brazilian agency CNPq.

REFERENCES

- [1] H. Schantz, *The Art and Science of Ultrawideband Antennas*, Boston: Artech House, 2005.
- [2] R. Aiello, A. Batra, *Ultra Wideband Systems: Technologies and Applications*, Oxford: Elsevier, 2006.
- [3] Z. N. Chen, M. Y. W. Chia, *Broadband Planar Antennas: Design and Applications*, New York: J. W. & Sons, 2006.
- [4] M. J. Ammann, "Square planar monopole antenna," in *Proc. 1999 IEE Nat. Conf. on Antennas and Propagation*, 1999, pp. 37–40.
- [5] C.-Y. Hong, C.-W. Ling, I.-Y. Tarn, and S.-J. Chung, "Design of a planar ultrawideband antenna with a new band-notch structure," *IEEE Trans. Ant. Propag.*, vol. 55, pp. 3391–3397, Jun. 2006.
- [6] D. Valderas, J. Legarda, I. Guitiérrez, and J. I. Sancho, "Design of UWB folded-plate monopole antennas based on TLM," *IEEE Trans. Ant. Propag.*, vol. 54, pp. 1676–1687, Jun. 2006.
- [7] K. Q. da Costa, V. A. Dmitriev, and L. de F. P. de Carvalho, "Numerical analysis by method of moment (MoM) of a rectangular monopole antenna with parasitic loop elements," in *Proc. 2007 Eleventh URSI Commission F Open Symposium on Radio Wave Propagation and Remote Sensing*, Rio de Janeiro, 2007.
- [8] A. M. Abbosh, and M. E. Bialkowski, "Design of ultrawideband planar monopole antennas of circular and elliptical shape," *IEEE Trans. Ant. Propag.*, vol. 56, pp. 17–23, Jan. 2008.
- [9] I. Makris, D. Manteuffel, R. D. Seager, and J. C. Vardaxoglou, "Modified designs for UWB planar monopole antennas," in *Proc. 2007 Loughborough Antennas and Propagation Conference*, 2007, pp. 249–252.
- [10] R. F. Harrington, *Field Computation by Moment Method*, New York: Macmillan, 1968.
- [11] <http://zeland.com>
- [12] C. A. Balanis, *Antenna Theory: Analysis and Design*, 3rd ed., New York: John Wiley, 2005.